Mapping the Heparin-binding Sites on Type I Collagen Monomers and Fibrils

James D. San Antonio,* Arthur D. Lander,‡ Morris J. Karnovsky,* and Henry S. Slayter§

*Department of Pathology, Harvard Medical School, Boston, Massachusetts 02115; ‡Department of Brain and Cognitive Sciences and Department of Biology, Massachusetts Institute of Technology, Cambridge, Massachusetts 02139; and §Laboratory of Structural Molecular Biology, Dana Farber Cancer Institute and Department of Cellular and Molecular Physiology, Harvard Medical School, Boston, Massachusetts 02115

Abstract. The glycosaminoglycan chains of cell surface heparan sulfate proteoglycans are believed to regulate cell adhesion, proliferation, and extracellular matrix assembly, through their interactions with heparin-binding proteins (for review see Ruoslahti, E. 1988. *Annu. Rev. Cell Biol.* 4:229–255; and Bernfield, M., R. Kokenyesi, M. Kato, M. T. Hinkes, J. Spring, R. L. Gallo, and E. J. Lose. 1992. *Annu. Rev. Cell Biol.* 8:365–393). Heparin-binding sites on many extracellular matrix proteins have been described; however, the heparin-binding site on type I collagen, a ubiquitous heparin-binding protein of the extracellular matrix, remains undescribed. Here we used heparin, a structural and functional analogue of heparan sulfate, as a probe to study the nature of the heparan sulfate proteoglycan–binding site on type I collagen. We used affinity coelectrophoresis to study the binding of heparin to various forms of type I collagen, and electron microscopy to visualize the site(s) of interaction of heparin with type I collagen monomers and fibrils. Using affinity coelectrophoresis it was found that heparin has similar affinities for both procollagen and collagen fibrils (K_d's ∿60–80 nM), suggesting that

functionally similar heparin-binding sites exist in type I collagen independent of its aggregation state. Complexes of heparin–albumin–gold particles and procollagen were visualized by rotary shadowing and electron microscopy, and a preferred site of heparin binding was observed near the NH₂ terminus of procollagen. Native or reconstituted type I collagen fibrils showed one region of significant heparin–gold binding within each 67-nm period, present near the division between the overlap and gap zones, within the "a" bands region. According to an accepted model of collagen fibril structure, our data are consistent with the presence of a single preferred heparin-binding site near the NH₂ terminus of the collagen monomer. Correlating these data with known type I collagen sequences, we suggest that the heparin-binding site in type I collagen may consist of a highly basic triple helical domain, including several amino acids known sometimes to function as disaccharide acceptor sites. We propose that the heparin-binding site of type I collagen may play a key role in cell adhesion and migration within connective tissues, or in the cell-directed assembly or restructuring of the collagenous extracellular matrix.

INTERACTIONS between heparan sulfate proteoglycans (HSPGs)[1] and collagen fibrils are thought to play important roles in cell adhesion (Koda et al., 1985; Piepkorn and Chapman, 1985), and in the formation of extracellular matrix structures such as basement membranes (Tsilibary et al., 1988, 1990; Koliakos et al., 1989). It has been shown that HSPGs, heparan sulfates, and heparin each bind to type I collagen fibrils (Stamataglou and Keller, 1982; Koda et al., 1985; Keller et al., 1986; LeBaron et al., 1989).

The high affinity interaction between HSPGs or heparin and type I collagen fibrils is not common to other glycosaminoglycans (Koda et al., 1985; LeBaron et al., 1989). Furthermore, the interaction is completely disrupted by high salt, suggesting a primarily electrostatic basis for the binding (Koda et al., 1985; Keller et al., 1986). It has also been demonstrated that the native character of the collagen triple helix is required for high affinity HSPG/heparin–type I collagen binding (Koda et al., 1985; Keller et al., 1986; San Antonio et al., 1992), and that the COOH-terminal triple helical fragment of type I collagen, as generated by vertebrate collagenase treatment, shows an apparently higher affinity for heparin than does the NH₂-terminal triple helical fragment (Keller et al., 1986). Aside from a requirement for triple helical structure, the features of the type I collagen fibril

---

1. *Abbreviations used in this paper:* ACE, affinity coelectrophoresis; HSPG, heparan sulfate proteoglycan; RGD, arginine-glycine-aspartic acid.

necessary for HSPG or heparin binding remain unknown. Thus, here we attempted to define the HSPG-binding sites on type I collagen, owing to the likely importance of these sites in the interactions between cell surfaces and type I collagen—one of the most abundant molecules of the extracellular matrix. Thus, in this manuscript we have characterized heparin-collagen interactions by affinity coelectrophoresis (ACE) and, using electron microscopy, sites of interaction were mapped for the binding of heparin-colloidal gold complexes to individual type I procollagen molecules and to both native and reconstituted type I collagen fibrils.

Materials and Methods

Collagen Preparations

Procollagen Type I. Procollagen type I was isolated as detailed (Olsen et al., 1976). Briefly, leg tendons were dissected from 17-d-old chick embryos, digested with trypsin and collagenase, and then the tendon fibroblasts were pelleted. Tendons from twelve dozen embryos yielded about 2×10^9 cells, which were placed in suspension culture for 6 h. Procollagen type I was isolated from the culture medium of the suspension cultures by ammonium sulfate precipitation with final protein yields of ∼1.5 mg observed. Procollagen type I purity was confirmed by SDS-PAGE analysis, and protein concentration was determined by amino acid analysis, performed by the Biopolymer Laboratory of the Brigham and Women's Hospital (Boston, MA).

Collagen Type I

Acid Soluble. Collagen from rat tail tendons was isolated as described (San Antonio et al., 1992). Briefly, tendons were subjected to three cycles of extraction/precipitation with 0.5 N acetic acid/7.5% NaCl, and purity was confirmed by SDS-PAGE.

Native. Tendons were removed from the tails of 5-10 Long Evans rats and were placed in 0.1 M Tris HCl, 0.1 M NaCl, pH 7.5, with 1 mM PMSF and 1 mM EDTA. All procedures were conducted at 4°C, and used the same buffer as detailed above. Tendons were rinsed several times in buffer, and were diced into pieces of ∼1 cm using a razor blade and scissors. The sample was suspended in 100 ml of buffer, and homogenized at high speed in a food processor. The collagen was pelleted at 1,000 g/10 min, and the supernatant discarded. The pellet was resuspended in 100 ml of buffer, and was homogenized for 5 min. Insoluble collagen was pelleted at 10,000 g/10 min, the pellet was discarded, and the supernatant passed through a thick layer of cotton gauze. The collagen was pelleted at 15,000 g/20 min, resuspended in 10 ml of buffer, then pelleted again at 15,000 g/20 min. The pellet was placed in <1 ml of buffer, dispersed by a brief sonication on ice, and samples were used in electron microscopy studies. Some samples were further treated with chondroitinase ABC. Fibril suspensions were diluted 1:5 in enzyme buffer, and were incubated with 0.05 U/ml chondroitinase ABC (Sigma Chem. Co., St. Louis, MO) for 3 h at 37°C (Koda and Bernfield, 1984). Afterwards, fibril samples were pelleted and rinsed 2× in homogenization buffer, and then used in electron microscopy studies.

Heparin

Heparin (grade I, porcine intestinal mucosa) was from Sigma Chem. Co. Heparin was substituted with tyramine at the polysaccharide's reducing end (San Antonio et al., 1993), radioiodinated to a specific activity of about 30,000 cpm/ng, and then radioiodinated low M_r ^{125}I-Tyramine-labeled heparin chains (^{125}I-Tyr-heparin) of M_r ≤6,000 were isolated by Sephadex G-100 chromatography (Laurent et al., 1978; Jordan et al., 1979; Rosenberg et al., 1979). Heparin-BSA-gold colloid (5-nM particles) was from Sigma Chem. Co., and BSA-gold colloid (5-nM particles) was from E. M. Sciences (Fort Washington, PA). All other reagents used for ACE experiments were as described (Lee and Lander, 1991).

ACE

Procollagen Type I. Procollagen samples were stored at 0.5-1.0 mg/ml in 0.05 M ammonium acetate/ammonium bicarbonate, pH 7.8, and were prepared for ACE as detailed for other soluble proteins (Lee and Lander, 1991).

Acid Soluble Type I Collagen. Acid soluble lyophilized collagen samples were dissolved in 0.5 N acetic acid at 2.4 mg/ml, with gentle stirring overnight at 4°C. Collagen was serially diluted in 0.5 N acetic acid. Samples were rapidly neutralized by the addition of an equal volume of 0.5 N NaOH, mixed with warm 2× concentrated electrophoresis running buffer and agarose, and then poured into agarose wells (San Antonio et al., 1992). Electrophoresis of ^{125}I-Tyr-heparin through agarose wells each containing one in a series of concentrations of protein was performed as described (Lee and Lander, 1991).

Reconstituted Fibrillar Type I Collagen. Lyophilized collagen samples were dissolved in 0.5 N acetic acid at 1.2 mg/ml, with gentle stirring overnight at 4°C. Collagen was then dialyzed against 0.02 M Na$_2$HPO$_4$ for 48 h at 4°C. After dialysis the collagen formed a fibrous white precipitate. The sample was then sonicated with a steel probe sonicator (Braunosonic 1510; B. Braun Biotech Intl., Melsungen, Germany) on ice with five pulses, with each lasting ∼5 s, and with each spaced ∼15 s apart from the next pulse to avoid warming and melting the collagen. After this treatment the sample formed a visually homogenous milky white suspension. The collagen was serially diluted into the same phosphate buffer. Samples were mixed with an equal volume of 2× ACE gel buffer salts, and then with an equal volume of 2× agarose, and poured into agarose wells. Electrophoresis of heparin through these gels was as described above.

Preparation of Samples for Electron Microscopy of Procollagen–Heparin–Gold Complexes

Procollagen was dialyzed into 0.2 M potassium borate buffer (pH 8.0). BSA-heparin-gold 5-nm colloid was centrifuged 30 min at 60,000 g and the pellet resuspended in a small volume of buffer. The procollagen and heparin-gold were mixed (25 μg of procollagen plus 0.25 ml of concentrated 5-nm heparin-gold), allowed to bind for 15 min at 25°C, and loaded into a Sepharose 4B column of 6.9-ml bed volume poured and equilibrated in 0.2 M (NH$_4$)$_2$ CO$_3$ (pH 8.25). In some cases the reaction mixture was fixed with glutaraldehyde before loading on the column. The column was eluted at ∼5 ml/h and fractions of 0.2 ml were collected and analyzed by electrophoresis for protein, and by measuring A$_{520}$ to monitor heparin-gold content. Generally the first three fractions after the void volume were used for electron microscopy. Samples were prepared for electron microscopy as described by Margossian et al. (1991).

Electron Microscopy of Procollagen

Approximately 20-μg/ml solutions of complex were mixed with 0.25 vol of glycerol, sprayed on to freshly cleaved mica, dried in vacuo for 20 h, and rotary shadowed with platinum or tungsten by means of resistive or electron bombardment heating, respectively (Slayter, 1976, 1983). The estimated average metal-film mass thickness was 100 ng/cm^2 for tungsten and somewhat more for platinum. Samples were examined in the JEM 100CX electron microscope, using a top entry stage voltage with a 40-μm objective aperture, and at 100 kV acceleration voltage. Most micrographs were recorded at a magnification of 20,000× and enlarged photographically to 50,000 or 100,000×. High resolution darkfield images were also obtained, from the lightly shadowed specimens, by using matched annular condenser and objective apertures (Slayter, 1989, 1991).

Electron Microscopy of Fibrous Collagen

Reconstituted and native type I collagen fibrils were prepared as detailed above. Specimens of fibrous collagen were deposited on carbon-filmed grids, incubated at 4°C with heparin-gold for 30 min, washed with 0.1 M cacodylate buffer, pH 7.4, fixed 5 min with 0.25% glutaraldehyde in 0.1 M cacodylate buffer at pH 7.0, washed 3× with water, and then stained with 1% uranyl acetate without thorough poststain washing (Slayter, 1983). Calibration was based on micrographs of grating-replica standards and of Indanthrene Olive crystals (Labaw, 1964).

Electron Microscopy of Frozen Sections

Blocks of rat tail tendon (0.5 mm) were fixed for 1 h in 0.1% glutaraldehyde in Stefanini (1967) fixative (4% paraformaldehyde, 15% saturated in neutralized picric acid). Tissue blocks were then immersed overnight at 4°C in PBS containing 2.3 M sucrose. These were maintained in a liquid nitrogen refrigerator until use, for a minimum of 24 h. Specimen blocks mounted on cutting stubs were removed and sections were obtained with thickness ∼60 nm. The methods used are essentially those of Tokoyasu and coworkers (Tokoyasu and Singer, 1976; Tokoyasu et al., 1983) as modified by Watkins
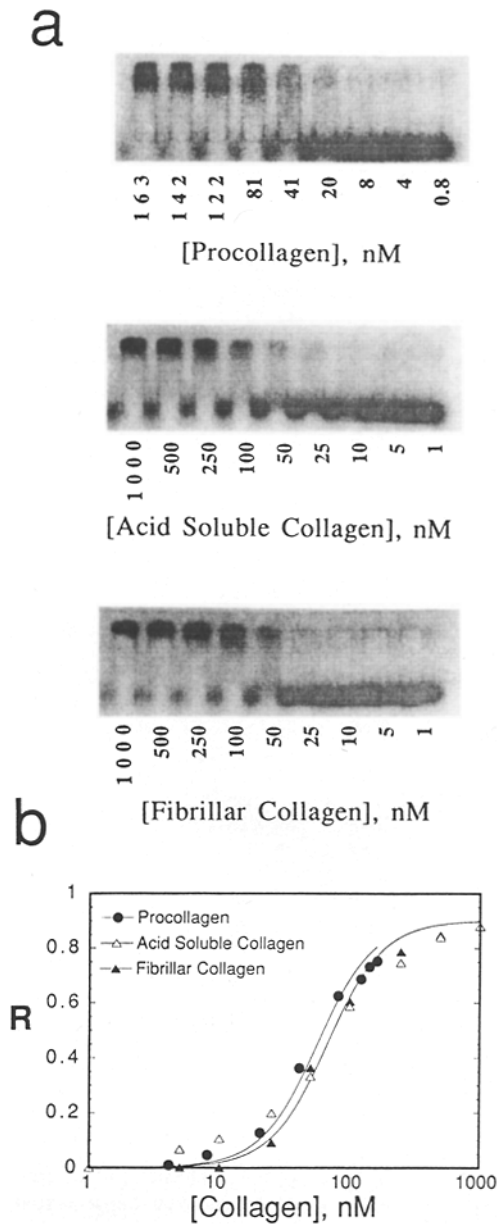
a

[Procollagen], nM

163 142 122 81 41 20 8 4 0.8

[Acid Soluble Collagen], nM

1000 500 250 100 50 25 10 5 1

[Fibrillar Collagen], nM

1000 500 250 100 50 25 10 5 1

b

Figure 1. (*a*) ACE analysis of the interactions between low M_r ^{125}I-Tyr-heparin and various forms of type I collagen. ACE gels were constructed containing type I collagen in the procollagen, acid solubilized, or reconstituted, fibrillar form. Collagens were present in gel lanes at the concentration (*nM*) indicated beneath each lane, with M_r's taken to be 450 K for procollagen, and 300 K for the other forms. Radiolabeled heparin was loaded into a sample slot (located above each gel), and electrophoresis was conducted towards the anode (located below each gel). Images of heparin migration patterns within ACE gels were obtained using a phosphorimager (Molecular Dynamics). From these electrophoretograms, the dissociation constant (K_d) can be estimated from the protein concentration at which the heparin is half-shifted from being fully mobile at very low protein concentrations or between protein-containing lanes, to being maximally retarded at high protein concentrations (Lee and Lander, 1991). (*b*) Calculation of affinities of low M_r heparin for different forms of type I collagen. Radiolabeled heparin was subjected to ACE analysis against the various collagen preparations as illustrated in (*a*). Heparin retardation coefficients (*R*) within each collagen-containing lane were determined (see Materials and Methods) and are plotted against protein concentration. Smooth curves represent nonlinear least-squares fits to the equation $R = R_\infty/(1 + K_d/[\text{protein}]^2)$.

et al. (1990). Thin sections were cut with a Reichert Ultracut Ultramicrotome fitted with an FC4D cryochamber (Vienna, Austria) at a temperature range of −110 to −130°C. The sections were mounted on Formvar/carbon-coated 200-mesh inch⁻¹ grids and labeled as previously described (Geuze et al., 1981). Sections were labeled by 30-min incubations with heparin-gold at ~60 μg/ml, washed, counterstained with uranyl acetate, and embedded in 1.25% methylcellulose as previously described (Watkins et al., 1991). Sections were examined with a JEOL 100CX electron microscope at 20,000× using a 40-μm objective aperture (JEOL U.S.A. Inc., Peabody, MA).

Results

Binding of Heparin to Different Forms of Type I Collagen

The binding interaction of heparin with monomeric and fibrillar collagen was studied using ACE. Type I collagen was incorporated into ACE gels in the following forms: procollagen type I (collagen monomers); reconstituted, acid-solubilized type I collagen, and reconstituted, fibrillar type I collagen. Electrophoresis of ^{125}I–Tyr–heparin was conducted through the collagen-containing lanes of ACE gels and electrophoretograms are shown in Fig. 1 *a*. Retardation coefficients (*R*) of the heparin migration fronts within each ACE gel lane were measured, and are plotted versus protein concentration (Fig. 1 *b*). From these curves the apparent average K_d's of the binding between heparin and the collagen preparations were derived. In two experiments, apparent K_d's (in nM) for heparin binding were: procollagen, 58 ± 2; acid soluble collagen, 79 ± 16; fibrillar collagen, 79 ± 14. These data indicate that the apparent affinities exhibited by each of the collagen preparations for heparin are not significantly different from each other. Furthermore, these affinities are in the range of those exhibited by other heparin-binding proteins for heparin (Lee and Lander, 1991; San Antonio et al., 1993).
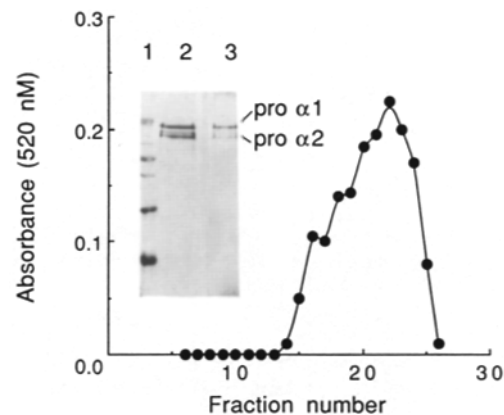

Figure 2. Chromatography of procollagen heparin–gold complexes on a Sepharose 4B column. Graph shows the elution of the heparin–gold reagent as determined by measuring A₅₂₀ of column fractions. Void volume is at fraction 14. (*Inset*) Procollagen content of column fractions was monitored by PAGE, followed by silver staining. Lane *1*, standards including 5 bands of highest staining intensity represent proteins of M_r 200, 116, 97, 66, and 45 K; lane *2*, ~1.0 μg procollagen type I from stock solution; lane *3*, procollagen from column fraction 17, representing about 5% of protein in fraction. Pro α1 and pro α2 chains of procollagen molecules are indicated. Specimens for electron microscopy were taken generally in the range from fractions 16 to 22.
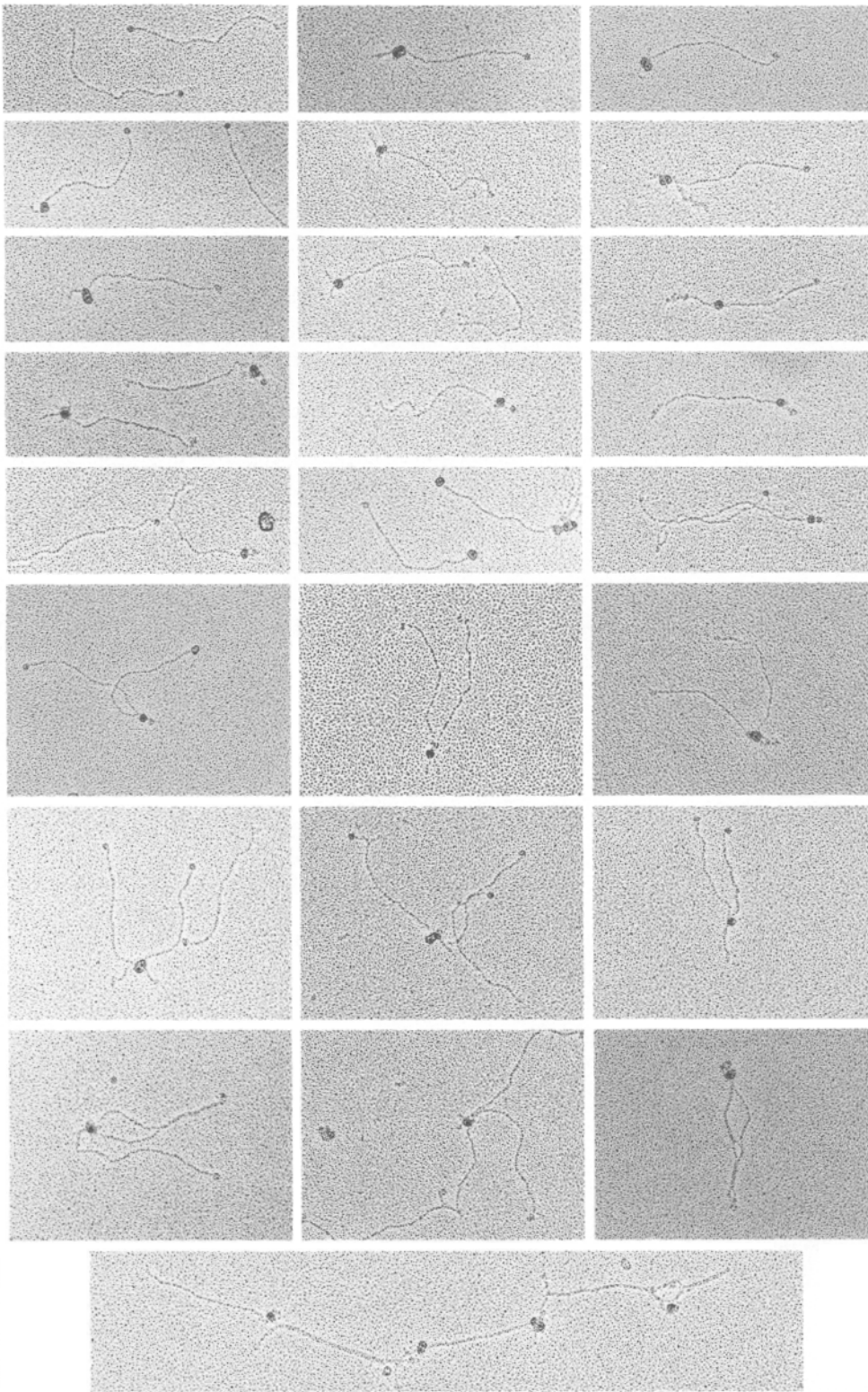
Figure 3. Electron micrographs of procollagen heparin–gold complexes showing procollagen (1st frame) and a variety of complexes observed by rotary shadowing. The first five rows of micrographs show monomolecular complexes between procollagen and heparin–gold. Micrographs in rows six through nine show complexes of procollagen molecules held together at one or more positions by heparin–gold. Bottom row width, 1500 nm.

Visualization of Heparin-binding Sites on Type I Collagen Monomers and Fibrils

Mapping of Procollagen. To map the heparin-binding site on collagen monomers, electron microscopy was used to examine complexes between heparin–gold reagent and procollagen in solution. Rotary-shadowed preparations were made of the material obtained from the excluded volume of the gel filtration step used to separate unbound heparin–gold from that which is complexed with the procollagen (Fig. 2). We obtained micrographs of the complex material mixed with unbound procollagen. In the course of these experiments it was discovered that the fraction excluded at the column-void
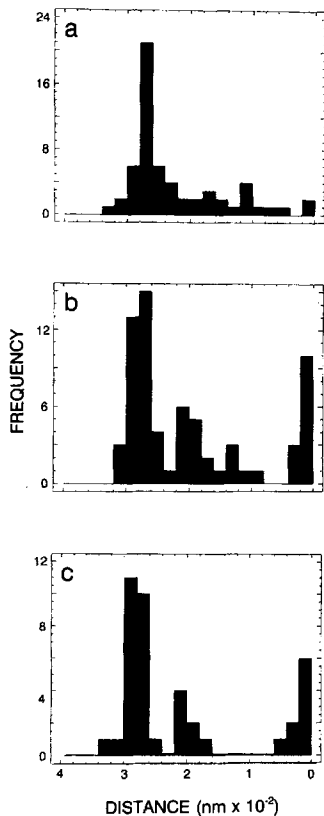
Figure 4. Histograms show mapping of the positions of heparin–gold on procollagen molecules in rotary-shadowed preparations of molecular complexes. Position of heparin–gold particles was measured from the center of the COOH-terminal globular head towards the NH₂ terminus of procollagen. Molecular complexes were fixed in: (*a*) 0.01%; (*b*) 0.0001%; (*c*) 0.00002% glutaraldehyde before column chromatography and rotary shadowing. In all cases there is a principle high frequency position of heparin–gold attachment at ∼300 nm from the center of the COOH-terminal head of procollagen.

Table I. Summary of Heparin–Gold–Procollagen EM Mapping Data

Experi-ment	GA Concen-tration %		Histogram peaks	
			*nm**	
1	0		195 maj	290 min
2	0	20	–	260 maj
3	.00002	Head/10 maj	–	280 maj
4	.0001	Head/10 min	–	280 maj
5	.01	–	–	280 maj
6	.01	–	–	290 maj

* Distance in nm from COOH terminus, or center of head, in procollagen, to center of heparin–gold marker.
GA, glutaraldehyde; maj, major peak; min, minor peak (collagen = 328 nm in same experiment).

volume (fraction 17) contained a large proportion of large intermolecularly cross-linked collagen complexes associated with some heparin–gold, but that individual procollagen complexes with heparin–gold reagent were rare. On the other hand, fraction 22 contained a much greater proportion of monomolecular complexes. Complexes representative of the variety encountered are shown in Fig. 3, including some containing more than one procollagen molecule. Procollagen is shown in Fig. 3 (*upper left*) with the characteristic 10-nm head. In the first five rows of selected micrographs of complexes of a single procollagen molecule with heparin–gold, the position of binding is clearly identified by the characteristic gold colloid particle with a dense core. In rows 6–9, complexes are illustrated in which procollagens are bound together by a single multivalent heparin–gold colloid particle. The positions of the heparin–gold particles on procollagen molecules were measured for complexes obtained under different experimental conditions. Fig. 4 summarizes the location of heparin–gold particles in several representative experiments as a function of their position relative to the center of the COOH-terminal head of procollagen. The histograms show a principal peak of heparin binding near the NH₂ terminus of procollagen. Quantitative results are summarized in Table I.

To stabilize complexes, we subjected them to glutaraldehyde fixation, using a series of glutaraldehyde concentrations, buffered to neutrality. The fixation reaction was stopped by adding an excess of glycine to block unbound glutaraldehyde, thus minimizing both intramolecular cross-linking between procollagen molecules and background due to possible nonspecific cross-linking between the heparin–gold and procollagen. Preferred regions of heparin–gold

binding were found in all of the experiments (Fig. 4), and the data are summarized in Table I. Most of the heparin–gold is found at a site very near the tail end of the molecule. The peak at ∼10–20 nm from the head, is somewhat suppressed at the higher glutaraldehyde concentrations (Fig. 4, *a* and *b*), but the other peak ∼290 nm from the head (very near the tail end), is always maintained (Fig. 4). Validity of these results was supported by a control experiment in which bovine serum albumin complexed with gold was used in mapping experiments and failed to bind to procollagen (data not shown).

Mapping of Reconstituted Collagen Fibrils. Our finding of one preferred heparin-binding site on procollagen monomers led us to determine if heparin-binding sites are also available in the type I collagen fibril, which is a structure composed of overlapping collagen monomers. Thus, mapping experiments were undertaken with several forms of fibrous collagen. Labeled fibrils were selected and scored for the position of the heparin–gold particles in relation to the 67-nm repeat of native-type fibrils, measuring from the beginning of the overlap zone (Fig. 5 *c*, *arrow*) toward the gap zone. Fig. 5 *c* shows a typical type I collagen fibril heavily labeled with heparin–gold in the region of the "a" bands. The data were plotted as histograms and are shown in Fig. 6. A single major peak is clearly evident in Fig. 6 *a* at a position ∼35 nm from the origin, with a possible minor peak at 65 nm. No other significant hot spot is seen in this profile. The experiment was repeated several times and, always, major peaks at ∼30–35 nm were found as indicated in Table II.

Mapping of Native Collagen Fibrils. We next tested whether the heparin-binding sites we observed in reconstituted collagen fibrils might be available for heparin binding in native fibrils in vivo, by examining heparin–gold binding by native collagen not only in preparations of homogenized rat tail tendon, but also in frozen sections of rat tail. Isolated native fibrils from homogenized tendon, and frozen sections of unfixed rat tendon when stained with heparin–gold, showed a major peak at ∼30 nm from the head and a minor peak at ∼62 nm from the head (Fig. 6, *b* and *c*). Table II summarizes the results of a number of different experiments. A control experiment was performed in which the access of heparin–gold was blocked by the presence of heparin (∼200 μg/ml). Under these conditions the major peak of heparin–gold binding at the center of the molecule virtually disappeared.

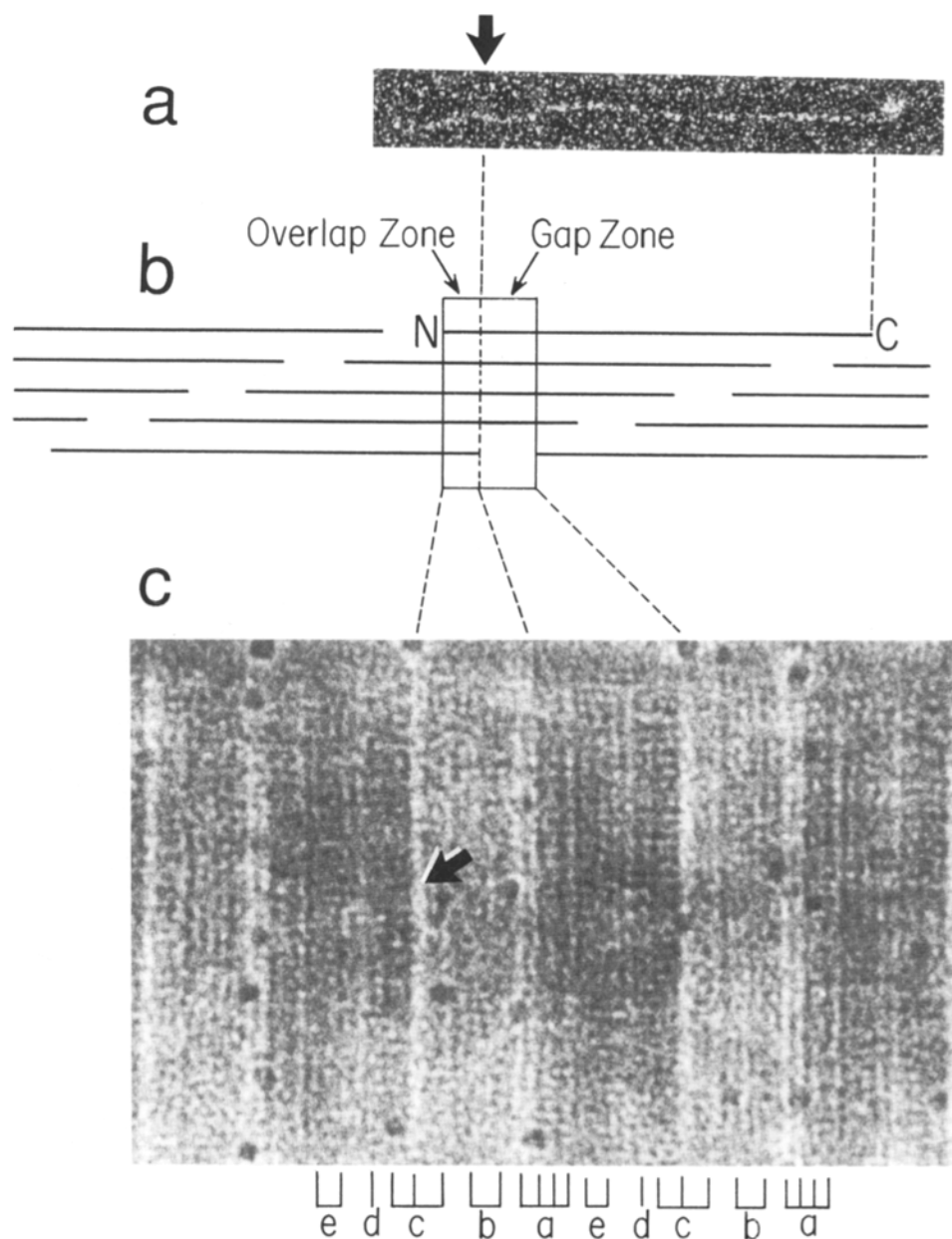*Effect of Chondroitinase upon Mapping of Native Colla-*

Figure 5. Composite correlating data obtained for the binding of heparin–gold to procollagen type I and to collagen type I fibrils. (*a*) Darkfield electron micrograph of tungsten rotary-shadowed preparation of procollagen showing globular COOH-terminal head on right, and position of putative heparin binding site (*black arrow*) as deduced by mapping data in Fig. 4. The location of the COOH-terminal end of tropocollagen and of the preferred heparin-binding site relative to the molecular overlap model of the collagen fibril is indicated by the dotted lines. (*b*) Diagram showing the arrangement of tropocollagen monomers within the collagen fibril, relative to the location of the overlap and gap zone fibril staining pattern. This molecular model was proposed by Chapman (1974). Tropocollagen molecules are shown as horizontal rods, and the polarity of all monomers in the fibril is indicated by N (NH$_2$ terminus) and C (COOH terminus) markings on one monomer. A diagram of the molecules within one 67-nm period (boxed area) is also shown expanded in Fig. 7. (*c*) Electron micrograph of glutaraldehyde-fixed, heparin-gold type I collagen fibril complexes, in fibrils visualized by uranyl acetate staining. Letters below micrograph show positions of positively stained fibril bands, following the accepted notation (Gross and Schmitt, 1948). Dotted lines between molecular model in *b* and the electron micrograph show corresponding overlap and gap zones. The location of heparin–gold particles relative to the molecular structure of the fibril as presented in Fig. 6 was measured within each 67-nm period, beginning at the center of the left border of the overlap zone (origin, *arrow*), and extending to the center of the right border of the gap zone. Heparin–gold particles appear as circular dark objects present mainly in the "a" bands region of the fibrils.

gen Fibrils. In another series of experiments the heparin–gold-binding site of native rat tail type I collagen was mapped before and after treatment of the collagen fibrils with chondroitinase. It was thought that chondroitinase treatment might uncover sites on collagen fibrils that are masked by endogenous proteoglycans such as decorin, thus making mapping of heparin-binding sites more definitive. In two experiments, the primary binding site was ~30 nm from the head. A second minor site at ~65 nm became somewhat more discrete after the chondroitinase treatment, but overall, chondroitinase treatment of fibrils had little effect on heparin–gold binding to fibrils. Table II shows histograms summarizing the data from these experiments. Since seg-

ment long spacing preparations of type I collagen are formed at low pH in acetic acid, and heparin–gold is unstable under these conditions, mapping experiments were found not possible to conduct on segment long spacing fibrils.

For the mapping experiments, the potential error in assigning positions on the basis of the heparin–gold label procedure is dependent upon several factors. First, the albumin–heparin–gold complex is ~10 nm in diameter. (The complex is visualized to be 10 nm in the metal-coated molecular preparations but only the 5-nm gold core is visualized in the fibrillar preparations.) Second, this marker could attach from the left, right, above, or below relative to the actual binding site. Third, some shrinkage upon dehydration (up to
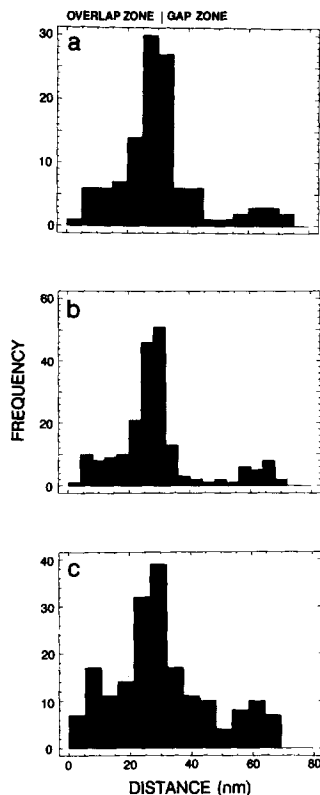
OVERLAP ZONE | GAP ZONE

DISTANCE (nm)

Figure 6. Histograms show mapping of the positions of heparin–gold on (*a*) reconstituted type I collagen fibrils; (*b*) native fibrils from homogenized rat tail tendons; (*c*) fibrils in frozen sections of native rat tail tendon. The location of heparin–gold particles relative to the molecular structure of the fibril (see Fig. 5) was measured within each 67-nm period, beginning at the center of the left border of the overlap zone, and extending to the center of the right border of the gap zone. In all cases there is a principal high frequency position of heparin–gold attachment at ~30 nm from the beginning of the overlap zone toward the gap zone, in the "a" (see Figs. 5 *c* and 7) bands region of the fibril.

Table II. Summary of Heparin–Gold–Collagen Fibril EM Mapping Data

Experiment	Description	Histogram peak
		nm
7	Reconstituted collagen	30
8	Reconstituted collagen	32
9	Reconstituted collagen	30
10	Native collagen fibrils	30
11	Chondroitinase treated; native collagen fibrils	30
12	Native fibrils	27
13	Chondroitinase treated; native collagen fibrils	27
14	Frozen section of nonfixed rat connective tissue	27

10%) may be expected in procollagen. Finally, markers may detach slightly prior to or during fixation. However, the data show a number of rather narrow (10 nm, two histogram bars) histogram maxima peaks. It is thus concluded that all factors mentioned other than the marker size must be of lesser importance and suggest that the error is roughly the size of the marker.

Discussion

Here, we have explored the nature of heparin binding by type I collagen monomers and fibrils. In the first series of electron microscopy experiments, heparin binding to type I procollagen was studied, as procollagen remains in the monomeric state. Since procollagen retains its COOH-terminal globular head, the polarity of the molecules can be readily identified. Histograms of procollagen–heparin–gold mapping experiments include data from complexes that were unfixed as well as complexes fixed using three different glutaraldehyde concentrations. In all cases there was a preferred site of attachment of heparin–gold near the NH$_2$-terminal end, positioned ~290 nm from the head–neck juncture of the procollagen molecule. In addition, in several preparations there was evidence of other apparently weaker sites that appear at lower concentrations of glutaraldehyde, or in the absence of fixation, at the COOH-terminal end, or at a position ~10–20 nm from the COOH-terminal end, starting from the head–neck junction. It is interesting that the COOH-terminal binding site is missing in the preparations of complexes which were fixed at high concentrations of glutaraldehyde, suggesting that glutaraldehyde treatment has eliminated that site either by amino derivitization or by modifying collagen conformation.

The principle heparin-binding site on type I collagen

fibrils was found near the interface between the overlap and gap region in the vicinity of the "a" bands as shown in Fig. 6. Experiments substantiated that this heparin-binding site occurs in this same position in reconstituted type I collagen fibrils, as well as in those of native tissue, and in fibrils from homogenized rat tail tendons. The correlation between the results from the mapping of the heparin-binding site on procollagen with that of fibrils was facilitated using the overlap model presented by Chapman, 1974 (Fig. 5). In this model, the "a" bands contain elements of the NH$_2$ terminus. Therefore, our finding that heparin attaches primarily to site(s) near the NH$_2$ terminus of procollagen is compatible with the presence of a preferred binding site located near the division between the overlap and the gap zone in the fibrils, in the "a" bands region (see Fig. 5). All of the results with monomolecular complexes were obtained with type I procollagen obtained from chicken tendon fibroblasts. However, the experiments on fibrils used both native-type I collagen fibrils, and purified reconstituted native-type collagen fibrils from rat tail tendon. Given that the structural features of type I collagen are highly conserved, the comparison is most likely valid (Monson et al., 1982).

It is important to determine the level of structural organization of the collagen fibril required for high affinity heparin binding. Previous work has shown that monomeric tropocollagen binds heparin (Obrink, 1973), and that disrupting the triple helical conformation by melting of the collagen significantly reduces its heparin-binding affinity (Koda et al., 1985; Keller et al., 1986; San Antonio et al., 1992). In this report we have shown that type I procollagen and fibrillar type I collagen display similar binding affinities for low molecular weight heparin. Our finding that heparin-binding sites are available for the binding of heparin–gold not only in reconstituted collagen fibrils, but also in native collagen fibrils, which are complex structures composed of types I, III, and V collagen molecules, is also considered significant. In principle, one might expect fibrillar collagen to exhibit a higher apparent affinity than procollagen for heparin, since fibrils are potentially multivalent ligands. The fact that a higher apparent affinity was not seen suggests that any improvement in binding affinity due to multivalency is effectively offset in fibrils by a decrease in numbers of binding sites that are available. Such a decrease is expected, in fact, since a significant fraction of the collagen monomers in a

fibril are thought to be buried beneath the surface, and presumably unavailable for binding.

Others have reported that when vertebrate collagenase was used to cleave type I collagen, the COOH-terminal fragment bound to a heparin affinity column more tightly than did the larger NH$_2$-terminal fragment (Keller et al., 1986). This is contrary to our finding of a preferred binding site near the NH$_2$ terminus, but there are ways in which this discrepancy may be explained. For example, it is possible that a cryptic heparin-binding site in the COOH-terminal region of type I collagen is made accessible for heparin binding only after collagenase treatment. Alternatively, differences in the characteristics (e.g., size, multivalency) of the heparin–gold reagent used in the present study and the affinity matrix used by Keller et al. (1986), may give rise to differences in accessibility of heparin-binding sites to these two reagents.

It has been proposed that heparin-binding sequences in many proteins consist of clusters of three to five basic amino acids, interspersed with hydropathic amino acids, and present within an α helical conformation (Cardin and Weintraub, 1989). When we searched the complete sequences of the α1 and α2 chains of human type I procollagens (Kuivaniemi et al., 1988; Tromp et al., 1988) for such consensus sequences, none were found. Thus it appears that type I collagen uses novel types of binding sites to interact with heparin and HSPGs. As an approach to identifying the heparin-binding sites on type I collagen, we examined our data showing that the primary heparin-binding site on procollagen is located near the NH$_2$ terminus of the molecule, and that within the fibril the preferred heparin-binding site falls in the "a" bands region (see Figs. 5 c and 7). We inspected the amino acid sequences of the α1 and α2 chains of type I collagen in relation to the location of heparin binding we observed in the monomer and the fibril. In these regions of the collagen triple helices, we concentrated on locating amino acid sequences of net basic charge which might prove suitable as binding sites for the polyanion heparin. Interestingly, one highly basic sequence was found in the triple helix near the NH$_2$-terminal end of procollagen, as well as within the "a" band region of the fibril, and is present in type I collagens of human, bovine, rat, and chick (Kuivaniemi et al., 1988; Hulmes et al., 1973; Tromp et al., 1988) (Fig. 7). This locus consists of nine basic amino acids, six of them contributed by the α1 chains, and three by the α2 chain, as shown below:

α1: hlys-gly-his-arg-gly-phe
α2: hlys-gly-ile-arg-gly-his

In the α1 chain of rat tropocollagen, this site includes amino acid residues 87–92 (Hulmes et al., 1973). Three of the basic amino acids within this sequence are hydroxylysine residues, which are involved in cross-links, and which sometimes function as dissacharide acceptor sites (Butler and Cunningham, 1965, 1966). We propose that this domain may function as a heparin-binding site in type I collagen. It should be stressed that there are other clusters of basic amino acids located in the collagen triple helices constituting the "a" band fibril region, but these all include fewer basic amino acids than the site discussed above, and often are present in close proximity to triple helical domains carrying strong negative charges (Fig. 7).

In the type I collagen monomer one other highly basic domain exists in the triple helix near the carboxy terminus (Fig.

7, arrow 7), and it also contains hydroxylysine residues involved in cross-links (Butler and Cunningham, 1966). The domain carries eight positive charges, and differs from the primary sequences of our proposed heparin-binding site, in both the composition and arrangement of some of its positively charged amino acids. It is possible that the weak heparin binding we observed near the COOH-terminal end of procollagen (Fig. 4, b and c) may be partially or wholly due to heparin binding to the COOH-terminal basic domain described above. In fact, this same site could be responsible for the heparin-binding affinity attributed to the COOH-terminal portion of type I collagen (Keller et al., 1986). The potential error in positioning the heparin–gold reagent relative to procollagen, however, makes it difficult at present to distinguish between binding of heparin–gold to the putative COOH-terminal heparin-binding sequence, as opposed to other basic domains near or on the globular head of procollagen.

It has been predicted that the proteoglycan-binding site should be in the "a" and "c2" band regions of the type I collagen fibril (see Figs. 5 c and 7), based on fibril staining patterns, as well as the concentration of unpaired positive charges of the combined rat and bovine sequences of the α1 chains (Doyle et al., 1975). It is significant in the present study that we observed heparin binding mainly to the "a" bands of native type I collagen. Previous work showed, however, that in tissues the location of various types of proteoglycans (e.g., dermatan and keratan sulfate PGs) on type I collagen fibrils is not limited to the "a" bands region, but can also occur within the "c," "d," or "e" bands regions (see Figs. 5 c and 7) of the 67-nm period (for review see Ruoslahti, 1988; Scott, 1988, 1991). Further work is necessary to determine if in vivo cell surface or extracellular matrix forms of HSPGs preferentially occupy the "a" bands region of type I collagen fibrils.

The relationships between the cell-attachment sites of type I collagen fibrils and heparin-binding sites are of great interest because heparin and syndecan-1 block cell adhesion to type I collagen in vitro (Koda et al., 1985; Piepkorn and Chapman, 1985). It is proposed that proteoglycans have this effect because they bind extracellular matrix molecules at sites that are adjacent to cell-attachment sites and thereby sterically hinder the binding of cell surface integrin receptors (Brennan et al., 1983).

The spatial relationship between the putative heparin-binding site and various potential cell-attachment sites on collagen fibrils are considered in Fig. 7. An average heparin molecule of 15,000 D is ∼30-nm long. If collagen-binding sites on heparin consist of randomly distributed pentasaccharide sequences (as do antithrombin III–binding sites [Marcum and Rosenberg, 1989]), then a locus on heparin of ∼2.5 nm could span the putative heparin-binding site on the collagen triple helix. In the collagen fibril, tropocollagen molecules are ∼300-nm long, the intermolecular spacing between them is ∼1.5 nm, and the length of one fibril repeat unit is ∼67 nm (Brodsky and Eikenberry, 1982). Thus, heparin molecules would not be long enough to span the distance between two heparin-binding sites of adjacent 67-nm periods (see Figs. 5 and 7). Heparin molecules would, however, be long enough to bind to a heparin-binding site on one tropocollagen helix, and span the distance between this site, and certain cell-attachment domains on adjacent tropocollagen monomers (e.g., Fig. 7, sites marked by arrows 2 and
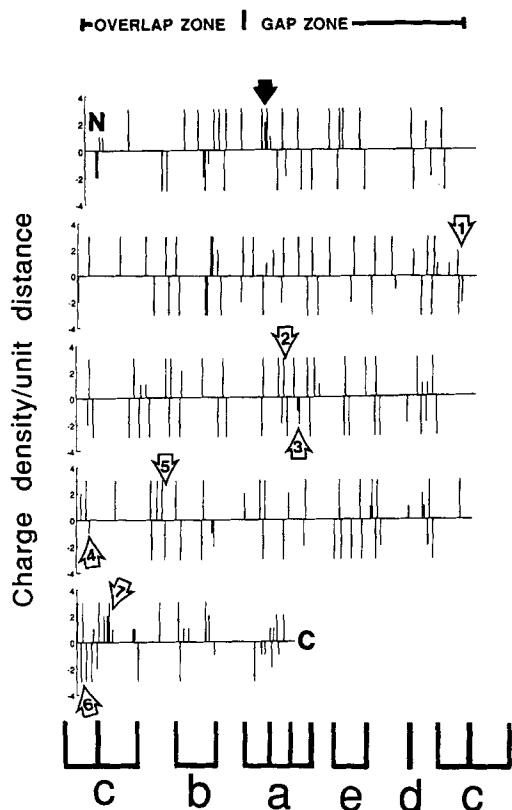
Figure 7. Diagram showing the charge density profiles of tropocollagen monomers within one 67-nm period of the type I collagen fibril, and the relative positions of the putative heparin-binding site and potential cell-attachment domains and argine-glycine-aspartic acid (RGD) sequences. The model of Chapman (1974) for the overlap of the α1 chains of rat type I collagen within the fibril was used as a guide to align the α1 chains of the human molecule, based on the high degree of sequence homology between the collagens of these species. The distribution of charged residues of the human protein matched nearly exactly with those of the rat, although it was necessary to delete several nonhomologous residues from the human sequence to achieve alignment. The fibril portion shown is an expanded diagram of the molecules within the boxed area of Fig. 5 b, and includes one overlap and one gap zone, as indicated. Horizontal bars represent segments of five overlapping triple helical tropocollagen molecules, with the NH₂ terminus (N) of one monomer located at the upper left of the diagram, and the COOH terminus (C) of another monomer at the lower right of the diagram; spacing between tropocollagen molecules is not to scale. Vertical bars represent total charge density at each residue unit along each triple helix, i.e., these values were determined by aligning the primary sequences of the human type I collagen α1 and α2 chains (Kuivaniemi et al., 1988; Tromp et al., 1988), and summing the charges of the three aligned residues across the chains of the triple helix. The location of the proposed heparin-binding domain is indicated (black arrow). Potential cell attachment sites and RGD sequences include DGEA (arrow 1) (Staatz et al., 1990, 1991) of the α1 chains of human, chicken, bovine, and rat; RGDA of the α1 chains of the human (arrow 2); RGDT of the α2 chain of the chicken but not human protein (arrow 3) (Dedhar et al., 1987; Pignatelli and Bodmer, 1988); RGDG of the α2 chain of the human (arrow 4); RGDQ of the α2 chain of the human (arrow 5); and RGDK of the α1 and α2 chains of the human (arrow 6) (see Hulmes et al., 1973; Bernard et al., 1983; Kuivaniemi et al., 1988; Tromp et al., 1988 for all sequences). Basic domain near COOH terminus showing sequence homology to proposed heparin-binding site (see Discussion) is indicated (arrow 7). Letters and bars at bottom of figure show positions of positively stained fibril band domains, following the accepted notation (Gross and Schmitt, 1948).

3), thereby potentially influencing cell–collagen interactions. The precise in vivo role of HSPGs as regulators of integrin receptor–collagen interactions will remain uncertain, however, until the locations of available integrin-binding sites on native type I collagen fibrils have been mapped.

It is of interest to speculate on the in vivo role of the heparin-binding site of type I collagen. Possibly, this site functions to join extracellular matrix PGs and collagen fibrils, to give structural support to certain connective tissues, or to control aspects of collagen fibrillogenesis (e.g., see Ruoslahti and Engvall, 1980; Vogel et al., 1984; Ruoslahti and Pierschbacher, 1987; Scott and Parry, 1992). Alternatively, the heparin-binding site of type I collagen may function in cell adhesion, as a primary matrix receptor for cell surface HSPGs (Koda et al., 1985; Sanderson et al., 1992). For example, via this binding site, cell surface HSPGs may act as coreceptors, by bringing extracellular ligands (e.g., collagen) together with high affinity cell surface receptors for these ligands (e.g., integrins) (see Bernfield et al., 1992 for review). Thus, given the abundance of HSPGs and type I collagen fibrils in most tissues, it is likely that the heparin-binding site on type I collagen participates in key physiological processes such as cell adhesion, migration, or cell-directed assembly or restructuring of the extracellular matrix.

References

Bernard, M. P., J. C. Myers, M. L. Chu, F. Ramirez, E. F. Eikenberry, and D. J. Prockop. 1983. Structure of a cDNA for the Proα2 chain of human type I procollagen. Comparison with chick cDNA for Proα2(I) identifies structurally conserved features of the protein and the gene. Biochemistry. 22:1139–1145.

Bernfield, M., R. Kokenyesi, M. Kato, M. T. Hinkes, J. Spring, R. L. Gallo, and E. J. Lose 1992. Biology of the syndecans: a family of transmembrane heparan sulfate proteoglycans. Annu. Rev. Cell Biol. 8:365–393.

Brennan, M. J., A. Oldberg, E. G. Hayman, and E. Ruoslahti. 1983. Effect of a proteoglycan produced by rat tumor cells on their adhesion to fibronectin-collagen substrata. Cancer Res. 43:4302–4307.

Brodsky, B., and E. F. Eikenberry. 1982. Characterization of fibrous forms of collagen. Methods Enzymol. 82:127–174.

Butler, W. T., and L. W. Cunningham. 1965. The site of attachment of hexose in tropocollagen. J. Biol. Chem. 240:3449–3550.

Butler, W. T., and L. W. Cunningham. 1966. Evidence for the linkage of a disaccharide to hydroxylysine in tropocollagen. J. Biol. Chem. 241:3882–3888.

Cardin, A. D., and H. J. R. Weintraub. 1989. Molecular modelling of protein-glycosaminoglycan interactions. Arteriosclerosis. 9:21–32.

Chapman, J. A. 1974. The staining pattern of collagen fibrils. I. An analysis of electron micrographs. Connect. Tissue Res. 2:137–150.

Dedhar, S., E. Ruoslahti, and M. D. Pierschbacher. 1987. A cell surface recep-

tor complex for collagen type I recognizes the Arg-Gly-Asp sequence. *J. Cell Biol.* 104:585–593.

Doyle, B. B., D. W. Hukins, D. J. Hulmes, A. Miller, and J. Woodhead-Galloway. 1975. Collagen polymorphism: its origins in the amino acid sequence. *J. Mol. Biol.* 91:79–99.

Geuze, H. J., J. W. Slot, D. A. Vanderle, and R. C. T. Scheffer. 1981. Use of colloidal gold particles in double-labeling immunoelectron microscopy of ultrathin frozen sections. *J. Cell Biol.* 89:653–665.

Gross, J., and F. O. Schmitt. 1948. The structure of human skin collagen as studied with the electron microscope. *J. Exp. Med.* 88:555.

Hulmes, D. J. S., A. Miller, D. A. Parry, K. A. Piez, and J. Woodhead-Galloway. 1973. Analysis of the primary structure of collagen for the origins of molecular packing. *J. Mol. Biol.* 79:137–148.

Jordan, R., D. Beeler, and R. D. Rosenberg. 1979. Fractionation of low molecular weight heparin species and their interactions with antithrombin. *J. Biol. Chem.* 254:2902–2913.

Keller, K. M., J. M. Keller, and K. Kuhn. 1986. The C-terminus of type I collagen is a major binding site for heparin. *Biochem. Biophys. Acta.* 882:1–5.

Koda, J. E., A. Rapraeger, and M. Bernfield. 1985. Heparan sulfate proteoglycans from mouse mammary epithelial cells. *J. Biol. Chem.* 260:8157–8162.

Koda, J. E., and M. Bernfield. 1984. Heparan sulfate proteoglycans from mouse mammary epithelial cells. *J. Biol. Chem.* 259:11763–11770.

Koliakos, G. G., K. K. Koliakos, L. T. Furcht, L. A. Reger, and E. C. Tsilibary. 1989. The binding of heparin to type IV collagen: domain specificity with identification of peptide sequences from αI(IV) and α2(IV) which preferentially bind heparin. *J. Biol. Chem.* 264:2313–2323.

Kuivaniemi, H., G. Tromp, M. Chu, and D. G. Prockop. 1988. Structure of a full-length cDNA clone for the preproα2(I) chain of human type I procollagen. *Biochem. J.* 252:633–640.

Labaw, L. W. 1964. Preparation of a 25-Å spacing crystal for magnification calibration above 18,000×. *J. Appl. Phys.* 35:3076–3079.

Laurent, T. C., A. Tengblad, L. Thunberg, M. Hook, and U. Lindahl. 1978. The molecular-weight-dependence of the anti-coagulant activity of heparin. *Biochem. J.* 175:691–701.

LeBaron, R. G., A. Hook, J. D. Esko, S. Gay, and M. Hook. 1989. Binding of heparan sulfate to type V collagen. *J. Biol. Chem.* 264:7950–7956.

Lee, M. K., and A. D. Lander. 1991. Analysis of affinity and structural selectivity in the binding of proteins to glycosaminoglycans: development of a sensitive electrophoretic approach. *Proc. Natl. Acad. Sci. USA.* 88:2768–2772.

Marcum, J., and R. D. Rosenberg. 1989. Role of endothelial cell surface heparin-like polysaccharides. *Ann. N.Y. Acad. Sci.* 556:81–94.

Margossian, S. S., J. W. Kreuger, J. R. Sellers, G. Cuda, J. B. Caulfield, P. Norton, and H. S. Slayter. 1991. Influence of the cardiac myosin hinge region on contractile activity. *Proc. Natl. Acad. Sci. USA.* 88:4941–4945.

Monson, J. M., J. Friedman, and B. J. McCarthy. 1982. DNA sequence analysis of a mouse proα1(I) procollagen gene: evidence for a mouse B1 element within the gene. *Mol. Cell Biol.* 2:1362–1371.

Obrink, B. 1973. A study of the interactions between monomeric tropocollagen and glycosaminoglycans. *Eur. J. Biochem.* 33:387–400.

Olsen, B. R., H. P. Hoffman, and D. J. Prockop. 1976. Interchain disulfide bonds at the COOH-terminal end of procollagen synthesized by matrix-free cells from chick embryonic tendon and cartilage. *Arch. Biochem. Biophys.* 175:341–350.

Piepkorn, M. W., and D. L. Chapman. 1985. Glycosaminoglycans and the substrate attachment of murine myeloma, 3T3, and cutaneous fibrosarcoma cells. *Lab. Invest.* 53:22–29.

Pignatelli, M., and W. F. Bodmer. 1988. Genetics and biochemistry of collagen binding-triggered glandular differentiation in human colon carcinoma cell line. *Proc. Natl. Acad. Sci. USA.* 85:5561–5565.

Rosenberg, R. D., R. E. Jordan, L. V. Favreau, and L. H. Lam. 1979. Highly active heparin species with multiple binding sites for antithrombin. *Biochem. Biophys. Res. Commun.* 86:1319–1324.

Ruoslahti, E. 1988. Structure and biology of proteoglycans. *Annu. Rev. Cell Biol.* 4:229–255.

Ruoslahti, E., and E. Engvall. 1980. Complexing of fibronectin glycosamino-

glycans and collagen. *Biochim. Biophys. Acta.* 361:350–358.

Ruoslahti, E., and M. D. Pierschbacher. 1987. New perspectives in cell adhesion RGD and integrins. *Science (Wash. DC).* 238:491–497.

San Antonio, J. D., A. D. Lander, T. C. Wright, and M. J. Karnovsky. 1992. Heparin inhibits the attachment and growth of balb/c-3T3 fibroblasts on collagen substrata. *J. Cell Physiol.* 150:8–16.

San Antonio, J. D., J. Slover, J. Lawler, M. J. Karnovsky, and A. D. Lander. 1993. Specificity in the interactions of extracellular matrix proteins with subpopulations of the glycosaminoglycan heparin. *Biochemistry.* 32:4746–4755.

Sanderson, R. D., T. B. Sneed, L. A. Young, G. L. Sullivan, and A. D. Lander. 1992. Adhesion of β lymphoid (MPC-II) cells to type I collagen is mediated by the integral membrane proteoglycan, syndecan. *J. Immunol.* 148:3902–3911.

Scott, J. E. 1988. Proteoglycan-fibrillar collagen interactions. *Biochem. J.* 252:313–323.

Scott, J. E. 1991. Proteoglycan: collagen interactions in connective tissues. Ultrastructural, biochemical, functional and evolutionary aspects. *Int. J. Biol. Macromol.* 13:157–161.

Scott, J. E., and D. A. Parry, 1992. Control of collagen fibril diameters in tissues. *Int. J. Biol. Macromol.* 14:292–293.

Slayter, H. S. 1976. High-resolution metal replication of macromolecules. *Ultramicroscopy.* 1:341–357.

Slayter, H. S. 1983. Electron microscopic studies of fibrinogen structure: historical perspectives and recent experiments. *Ann. N.Y. Acad. Sci.* 408:131–145.

Slayter, H. S. 1989. Secretion of thrombospondin from human blood platelets. *Methods Enzymol.* 169:251–269.

Slayter, H. S. 1991. High resolution shadowing. *In* Electron Microscopy in Biology. A Practical Approach. Oxford University Press, Oxford, U.K. 151–172.

Staaz, W. D., J. J. Walsh, T. Pexton, and S. A. Santoro. 1990. The α2B1 integrin cell surface collagen receptor binds to the α1 (l)-CB3 peptide of collagen. *J. Biol. Chem.* 265:4778–4781.

Staatz, W. D., K. F. Fok, M. M. Zutter, S. P. Adams, B. A. Rodriguez, and S. A. Santoro. 1991. Identification of tetrapeptide recognition sequence for the α2β1 integrin in collagen. *J. Biol. Chem.* 266:7363–7367.

Stamatoglou, S. C., and J. M. Keller. 1982. Interactions of cellular glycosaminoglycans with plasma fibronectin and collagen. *Biochem. Biophys. Acta.* 719:90–97.

Stefanini, M., C. De Martino, and L. Zamboni. 1967. Fixation of ejaculated spermatozoa for electron microscopy. *Nature (Lond.).* 216:173–174.

Tokoyasu, K. T., and S. J. Singer. 1976. Improved procedures for immunoferritin labeling of ultrathin frozen sections. *J. Cell Biol.* 71:894–906.

Tokoyasu, K. T., A. J. B. Dutton, and S. J. Singer. 1983. Immunoelectron microscopic studies of desmin (skeletin) localization and intermediate filament organization in chicken cardiac muscle. *J. Cell Biol.* 97:1736–1742.

Tromp, G., H. Kuivaniemi, A. Stacey, H. Shikata, C. T. Baldwin, R. Jaenisch, and D. J. Prockop. 1988. Structure of a full-length cDNA clone for the preproα1(I) chain of human type I procollagen. *Biochem. J.* 253:919–922.

Tsilibary, E. C., G. G. Koliakos, A. S. Charonis, A. M. Vogel, L. A. Reger, and L. T. Furcht. 1988. Heparin type IV collagen interactions: equilibrium binding and inhibition of type IV collagen self-assembly. *J. Biol. Chem.* 263:19112–19118.

Tsilibary, E. C., L. A. Reger, A. M. Vogel, G. G. Koliakos, S. S. Anderson, A. S. Charonis, J. N. Alegre, and L. T. Furcht. 1990. Identification of a multifunctional, cell-binding peptide sequence from the αI(NC1) of type IV collagen. *J. Cell Biol.* 111:1583–1591.

Vogel, K. G., M. Paulsson, and D. Heingard 1984. Specific inhibition of type I and type II collagen fibrillogenesis by the small proteoglycan of tendon. *Biochem. J.* 223:587–597.

Watkins, S. C., V. Raso, and H. S. Slayter. 1990. Redistribution of thrombospondin, von Willebrand's factor and fibrinogen during platelet aggregation and clot formation. *Histochem. J.* 22:507–518.

Watkins, S. C., H. S. Slayter, and J. F. Codington. 1991. Intracellular pathway of a mucin-type membrane glycoprotein in mouse mammary tumor cells. *Carbohydr. Res.* 213:185–200.